

Vol. 27 • No. 44 • November 25 • 2015

www.advmat.de

ADVANCED MATERIALS

WILEY-VCH

Continuous Fabrication of Hierarchical and Asymmetric Bijel Microparticles, Fibers, and Membranes by Solvent Transfer-Induced Phase Separation (STRIPS)

Martin F. Haase, Kathleen J. Stebe,* and Daeyeon Lee*

Classically, vigorous mixing of two immiscible liquids with appropriate stabilizers results in an emulsion, comprising one liquid phase dispersed in the other. Since particles strongly attach to interfaces, emulsions prepared with colloids are typically very stable,^[1] and have additional functionalities afforded by the particles themselves, with broad applications in coatings,^[2] cosmetics, pharmaceuticals^[3] and foods.^[4] The recent discovery of bicontinuous emulsion gels^[5,6] dramatically expands the possibilities of multiphase systems.^[7,8] These bicontinuous interfacially jammed emulsion gels, also known as bijels, are formed by arresting the spinodal decomposition^[9] of immiscible liquids with jammed colloidal particles at the interface.^[10] In contrast to conventional particle-stabilized emulsions, bijels have bicontinuous liquid architectures, making them ideal for applications that require intimate contact between two immiscible liquid phases or that rely on reaction or mass transfer through the interface. Bijels stabilized with catalytic nanoparticles, for instance, could function as crossflow microreaction media^[7] for biofuel upgrade reactions,^[11] enabling continuous mass transfer of reagents in and out of the structure and simultaneously allowing for interfacial catalysis and interphase mass transfer of reactants and products.

Despite these new opportunities, bijels prepared by the conventional method of thermal quenching are limited to privileged pairs of liquids and delicately prepared colloids,^[6,12,13] exhibit poor thermal stability, and are formed in batch processes, limiting their widespread application.^[8,14–16] Here, we describe the continuous generation of asymmetric and hierarchical bijels based on solvent transfer-induced phase separation (STRIPS). In STRIPS, phase separation is induced by extraction of a solvent from a homogeneous ternary mixture, and the bicontinuous morphology is stabilized by interfacial attachment of nanoparticles. STRIPS allows a much wider variety of immiscible liquid combinations and particles for bijel formation and enables continuous production of remarkably stable bijels. The formation of submicrometer domain sizes in STRIPS raises the interfacial area of bijels, facilitating efficient interphase mass transfer for various chemical separation processes. We demonstrate biphasic transport in bijels, which could be exploited for interfacial catalysis for diverse chemical reactions.^[17]

Alternatively, polymerization of STRIPS bijel materials generates planar or hollow fiber membranes with potential applications in filtration, as battery components, as sensors and as solid catalysts.^[14,16] The asymmetric and hierarchical structures generated by STRIPS complement the conventional bijels with uniform structure and further expand the potential of bijels by offering advantages in applications that require features of multiple length scales such as size selective transport and separations.^[18]

STRIPS requires the rapid injection of a homogeneous mixture of three liquids into a continuous phase. One of the liquids is a solvent that allows homogenous mixing of the other two liquids, (e.g., an oil and an aqueous phase), which are immiscible on their own. In the course of injection, this solvent is extracted into the continuous phase, leading to phase separation, in close analogy to the Ouzo effect.^[19] As a model system, we select diethylphthalate (DEP)^[20] as the oil phase; its refractive index differs from water, facilitating optical monitoring of the phase separation. We select ethanol as the solvent, and an aqueous suspension as the third liquid. The initial composition of this mixture is tuned to undergo spinodal decomposition via solvent removal when it is brought in contact with an aqueous phase.^[21,22] 22 nm silica nanoparticles, suspended in the ternary mixture along with a positively charged surfactant (cetyltrimethylammonium bromide (CTAB)), attach to the interface between the oil- and water-rich phases to arrest phase separation and stabilize the bicontinuous microstructure. CTAB aids nanoparticle dispersion in the ternary mixture and, more importantly, renders the nanoparticles partially hydrophobic via electrostatic adsorption (Figure 1a).^[23] During STRIPS, CTAB diffuses to the external water phase due to the concentration gradient (the concentrations of CTAB in the ternary mixture and the external aqueous phase are $>20 \times 10^{-3} \text{ M}$ and $1 \times 10^{-3} \text{ M}$, respectively); however, since the concentration of CTAB in the ternary phase is very large, we do not expect this mass transfer to significantly impact the efficacy of CTAB in making the nanoparticles hydrophobic. This strategy of in situ surface modification affords flexibility in the selection of colloids lacking in the traditional bijel fabrication route.^[24–28] Bijels, for example, can be prepared with positively charged silica nanoparticles modified in situ with an anionic surfactant (Figure 1a).

We demonstrate STRIPS by producing three types of bijel structures, namely microparticles, fibers, and membranes. The continuous production of bijel microparticles and fibers is realized within a device comprising two concentrically aligned cylindrical capillaries (Figure 1b) which also allows for optical imaging of the process. The dynamics of the phase separation can be monitored by tracking the evolving patterns of dark and bright contrast as the structures move through the

Dr. M. F. Haase, Prof. K. J. Stebe, Prof. D. Lee
Department of Chemical and
Biomolecular Engineering
University of Pennsylvania
Philadelphia, PA 19104, USA
E-mail: kstebe@seas.upenn.edu; daeyeon@seas.upenn.edu



DOI: 10.1002/adma.201503509

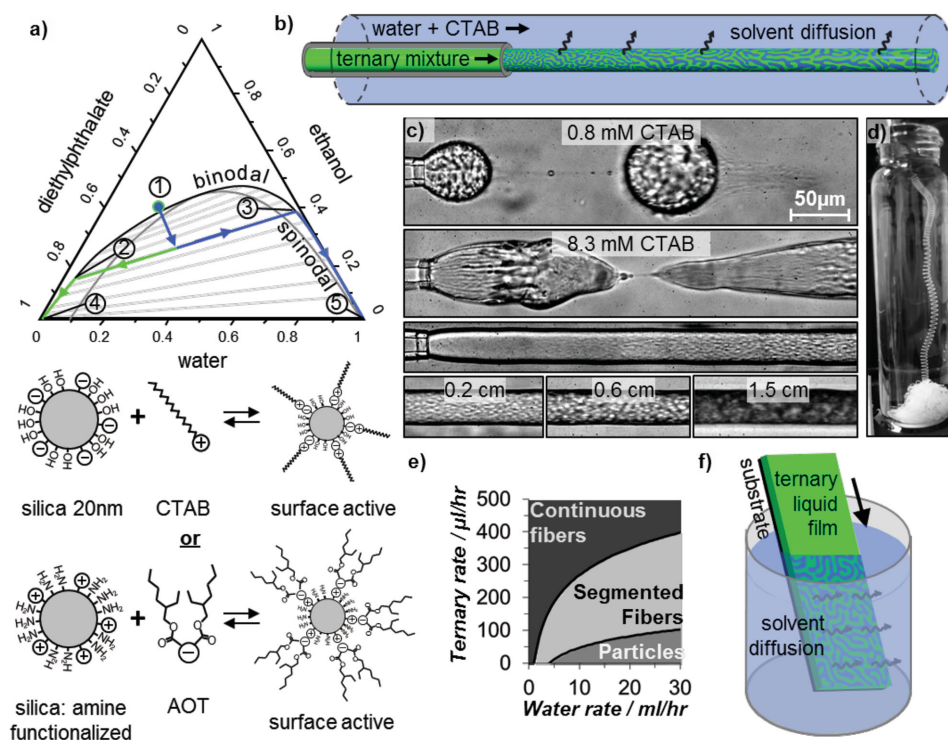


Figure 1. Bijel structure formation via STRIPS. a) Equilibrium phase diagram of the ternary liquid system comprising DEP, ethanol, and water (volume fractions). Arrows qualitatively depict the average compositional path, initiating at point 1 (41 vol% DEP, 41 vol% ethanol, 18 vol% H₂O) as a homogeneous ternary liquid mixture, progressing to points 2 and 3, and eventually to points 4 and 5 as the mixture phase separates owing to ethanol loss and water uptake. Below the phase diagram, the surface modification of silica nanoparticles by CTAB or of (3-Aminopropyl)trimethoxysilane functionalized silica by docusate sodium salt (AOT) is depicted schematically. b) Depiction of bijel fiber formation in a device made of concentrically aligned glass capillaries (diameters = 50 and 300 μm): The ternary liquid mixture containing CTAB and suspended nanoparticles flows as a jet from a nozzle into a water stream of pH 3 containing 1 × 10⁻³ M CTAB. c) Images of bijel microparticle and bijel fiber formation: high speed images of the ternary droplet-pinch off at low CTAB concentration, $c_{\text{CTAB}} = 0.8 \times 10^{-3}$ M, in the ternary mixture. (See SI-video 1, Supporting Information.) The image below shows the pinch off at elevated CTAB concentration, $c_{\text{CTAB}} = 8.3 \times 10^{-3}$ M, in the ternary mixture. Liquid jet at high flow rate of the ternary mixture (300 μL h⁻¹) and after polydiallyldimethylammonium chloride surface modification of the capillary. Below: images of the jet at different longitudinal positions. (See SI-video 1, Supporting Information.) d) Photograph of the collection of a continuous bijel fiber flowing out of the microfluidic device into a stagnant external aqueous phase. e) Operation diagram showing the effect of flow rate on the bijel structure formed in the capillary device. (SI-video 1 and Figure S11, Supporting Information.) f) Depiction of bijel membrane formation: A hydrophobic substrate is coated with a thin film of the CTAB and silica doped ternary mixture and subsequently immersed into a water bath.

device (Figure 1c). Bijel structure formation depends sensitively on relative flow rates, suspension composition and wetting conditions within the device. For example, injection of a suspension of the ternary liquid mixture with a CTAB concentration ($c_{\text{CTAB}} = 0.8 \times 10^{-3}$ M) and nanoparticle volume fraction ($\phi_{\text{NP}} = 0.042$) into a flowing aqueous stream leads to the formation of droplets which undergo transition to multiple emulsion droplets.^[21] By increasing c_{CTAB} , the droplet pinch off behavior changes dramatically (Figure 1c). Irregular, elongated droplets detach from the capillary orifice with evident phase separation patterns. The asymmetric drop shape evolution strongly suggests that the suspension is viscoelastic, which we attribute to the gelation and interfacial attachment of nanoparticles.^[29] These droplets form complex shaped bijel microparticles of nonuniform lengths as they flow through the device. To better regulate drop pinch off, control over the suspension wetting on the inner capillary is critical, and is achieved by coating the capillary with a cationic polyelectrolyte, poly(diallyldimethylammonium chloride). Thereafter, the suspension pinches off periodically to form particles of more uniform length at low flow rate, or forms a stable jet at higher

flow rate which becomes a bijel fiber with a constant diameter along the length of the channel (see Figure 1c).

The bijel structures formed, i.e., microparticles, segmented fibers, and continuous fibers, depend on the relative flow rates in the device, with higher ratios of inner to outer flow rates favoring higher aspect ratio structures (Figure 1e). The size of microparticles, and the length of segmented fibers can be tailored by varying the orifice diameter and the flow rate of the external water phase (see Figures S11–S13, Supporting Information), respectively. STRIPS bijel fibers of arbitrary length can be made by introducing a jet of the suspension into an otherwise stagnant vial of water; the fiber forms a curly structure owing to the so-called telephone cord instability (Figure 1d). Planar supported bijel membranes are formed in a closely related fashion by immersing a thin film of the ternary liquid mixture on a planar substrate into a water bath (Figure 1f). These liquid bijel structures show high thermal stability, retaining their structures up to at least 80 °C (Figure S14, Supporting Information).

The path of the compositional quench in STRIPS is illustrated qualitatively on the ternary phase diagram (Figure 1a). The

mixture is initially homogenous (point 1). Upon contacting the external phase, the abrupt loss of ethanol and concomitant uptake of water shifts the composition beneath the spinodal line, producing water- and DEP-rich phases (points 2 and 3). Since water is present in excess, ethanol is depleted continuously until the DEP-rich and water-rich phases attain compositions corresponding to the lower left and right corners of the phase diagram (points 4 and 5), respectively. STRIPS bijel formation is complementary in mechanism to well-established phase inversion techniques such as diffusion-induced phase separation (DIPS) widely used to produce porous hollow fibers or sheet membranes.^[30] In DIPS, nonsolvent is introduced into a homogenous mixture of polymer and solvent to initiate phase separation, whereas in STRIPS, solvent removal from a ternary mixture is the main factor that triggers the phase separation. Like DIPS, which has been implemented at large scales, STRIPS has significant potential for large-scale manufacturing of hierarchically structured bijels.

The surface and internal features of STRIPS bijel structures can be tuned to have a number of potentially important features. For example, the size of the surface pores and internal micropores can be tailored from several micrometers down to a few hundreds of nanometers, which has not been achievable in prior reports. These small pores likely give large specific surface areas to these STRIPS bijels. The configuration for micro-particle and fiber formation affords tremendous control over the structures' internal features, which can be varied from hollow to "structured" with interconnected water and oil networks. Mass transfer occurs nonuniformly across the jet radius, so different phase separation mechanisms (i.e., spinodal decomposition and nucleation and growth) likely occur in different regions, leading to the observed hierarchical and asymmetric microstructures. STRIPS bijel fibers typically have smaller pores on their surfaces and larger pores toward their centers. Asymmetric hierarchical pore structures are also evident in bijel membranes as shown in Figure 2a.

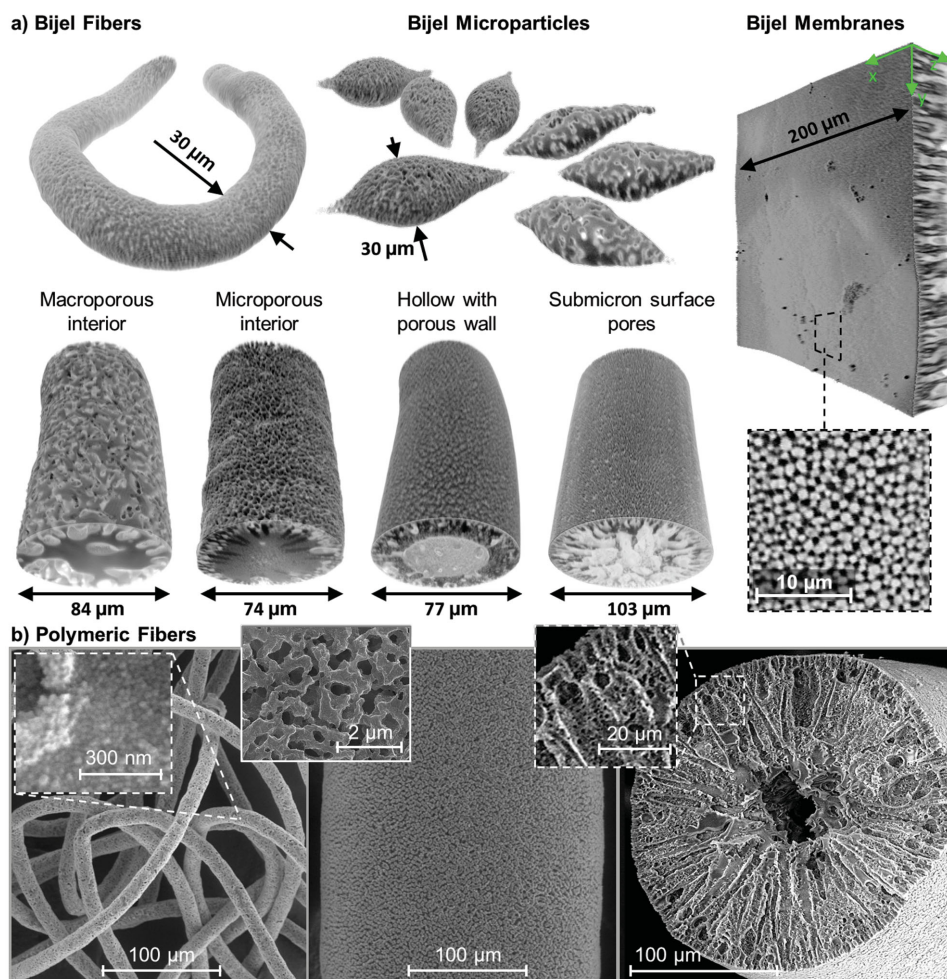


Figure 2. Hierarchical and asymmetric morphologies of bijel structures. a) Confocal microscopy images of bijel fibers, microparticles, and membranes with tunable surface and internal pore structure and size (see also SI-videos 2–5, Supporting Information). b) SEM images of surface structures of polymerized bijel fibers with 10 (left panel) and 250 μm (middle panel) diameter formed from 8 and 220 μm capillary orifices, respectively (Figure S13, Supporting Information, shows bijel microparticles with different sizes). The insets contain magnifications of the fiber surfaces showing the interfacially jammed silica nanoparticles (left) and the bicontinuous surface structures (middle). The right pane shows a cross-sectional view of a hollow bijel fiber with hierarchical wall features. The bicontinuous sub-domains of the fiber wall is magnified in the inset.

STRIPS affords broad flexibility in the selection of the oil phase, as hydrocarbons with a wide range of polarity, structure and functional groups can be formulated into homogenous ternary phases that undergo phase separation upon solvent removal. In fact, several hundred examples of such ternary mixtures exist and could potentially be used for bijel formation.^[31] We exploit this versatility by selecting polymerizable oils, 1,6 hexanedioldiacrylate (HDA) or butylacrylate (BA). The resulting bijel materials can be photopolymerized, and transferred to a refractive index-matching liquid, allowing imaging of their internal microstructure by confocal microscopy. Figure 2 shows reconstructed confocal images of fibers, microparticles, and membranes fabricated with different ϕ_{NP} and c_{CTAB} . All feature a uniform sponge-like surface structure supported by a porous substructure with either a continuous hollow core or a hierarchically structured scaffold.

SEM images of the polymerized bijel fibers reveal their remarkably hierarchical features, including surfaces decorated with interfacially jammed silica nanoparticles (inset, Figure 2b), cross-sections with radially aligned macropores and hierarchical pores arranged around a hollow core. This architecture strongly resembles that of fibers and membranes made via DIPS. However, in contrast to DIPS fibers, which require a bore fluid to form their core, the hollow cores of STRIPS bijel fibers form spontaneously as a consequence of the radially driven phase separation process. Its formation can be promoted or suppressed by controlling STRIPS parameters such as c_{CTAB} and ϕ_{NP} , as shown below.

The potential advantages of this hierarchical and asymmetric bijel architecture are manifold; the skin layer with tunable porosity can serve as the selective layer in membrane separation; a hollow fiber core can function as a drainage channel for liquids; the micropore infiltrated walls of the macrovoids offer large surface areas for interphase mass transfer; and the jammed nanoparticles could become catalytic materials promoting interfacial reactions.^[11,17]

We demonstrate the ability to tailor key fiber features such as pore size, specific surface area, and composition by selection of appropriate ϕ_{NP} and c_{CTAB} , using the HDA-water-ethanol system. Surface feature and pore size become finer, and specific surface area increases, with increasing ϕ_{NP} for a given c_{CTAB} (Figure 3a, rows), and with increasing c_{CTAB} at a fixed ϕ_{NP} (columns). In particular, surface pore size decreases asymptotically to a minimum (≈ 500 nm for $c_{CTAB} = 108 \times 10^{-3}$ M) with increasing ϕ_{NP} (Figure 3b). Interestingly, this trend differs from that in the typical bijel literature, for which a linear dependence on the $1/\phi_{NP}$ has been reported (Figure S17, Supporting Information), and may be attributed to the spatially nonuniform compositions during phase separation. In STRIPS, the fiber surface phase separates before its interior, with sufficient nanoparticles and surfactant present to promote particle attachment and to stabilize small features. Near the center of the fiber, however, the relative depletion of nanoparticles and surfactant allows phase separation to proceed further prior to arrest, favoring larger features. Alternatively, relatively high concentration of ethanol near the center of the fiber may delay interfacial nanoparticle jamming and allows phase separation to proceed further prior to arrest, favoring larger features. The water-to-oil domain volume ratio of the bijel fiber increases with ϕ_{NP} .

Counterintuitively, the water-rich phase forms the majority phase in most of the bijel fibers, in stark contrast to the initial ternary composition. The water-majority structures, particularly at higher ϕ_{NP} , we believe, are a result of the hindered transport of water and ethanol to the continuous phase due to large hydrodynamic resistance caused by small surface pores. This results in larger amounts of ethanol and water remaining trapped in the fiber phase after the completion of STRIPS.

The internal architecture of STRIPS bijel fibers can also be tailored by judicious selection of suspension conditions (Figure 3a), to range from separated-voids, to interconnected-voids with finger-like shapes, to a continuous channel extending throughout the fiber. At higher c_{CTAB} , aqueous subdomains form inside the internal oil structures (dashed boxes in Figure 3a); these subdomains change from separated voids to sponge-like interconnected voids with domain sizes of a few hundred nanometers with increasing c_{CTAB} . Similar subdomains appear in conventional bijels, attributed to secondary droplet nucleation, stabilized by off-neutral wetting of the constituent colloids.^[15] Their appearance in STRIPS bijels may rely on an analogous mechanism; the increase in c_{CTAB} may render the nanoparticles more hydrophobic, allowing water in oil emulsions to form. The sponge-like morphology found in our experiments at very high c_{CTAB} suggests that the secondary phase separation can also result via spinodal decomposition.

One of the most intriguing applications of bijels is their use as biphasic transport media.^[14] We demonstrate biphasic mass transfer in long-lived STRIPS bijels by preparing a bundle of aligned fibers and demonstrating permeation of polar and non-polar agents. We align the fibers by “printing” lines of bijel fiber as it emerges from the capillary orifice. We first test the stability of the bijel fibers in different aqueous media. Bicontinuous domains of STRIPS fibers made of DEP and water coarsened relatively rapidly, (in ≈ 120 min) in acidic conditions (pH 3), as highlighted by encircled regions in Figure 4a. In contrast, for basic aqueous phases (pH 9), no coarsening is evident even after 12 h (SI-video 7, Supporting Information). The mechanical stability of the fibers is also improved, as evidenced by their resistance to fracture under mild shaking of the container. We attribute this enhanced stability to strong silica particle aggregation resulting from higher CTAB adsorption on strongly charged silica nanoparticles.^[23,32]

With these aligned, stable bijel fibers, we confirm the bicontinuous structure by transporting agents of differing polarity through the two domains.^[14] The two ends of the fiber bundle are connected to two DEP reservoirs containing a hydrophobic fluorescent dye (Figure 4a). The fluorescent dye diffused through the oil-filled domain of the fibers over time; after 3 h, the entire DEP rich-domain is infiltrated by the dye. The structures remain robust, with no signs of coarsening for six additional hours. Thereafter, a hydrophilic fluorescent dye (Rhodamine 110) is added into the continuous aqueous phase. After a lag time, the dye distributes evenly throughout the water domains of the fiber as seen in Figure 4d. These results clearly demonstrate that bijel fibers can transport agents of opposite polarities through the corresponding domains while remaining robust for extended time periods.

In summary, we present a scalable method for continuous fabrication of hierarchically and asymmetrically structured bijel

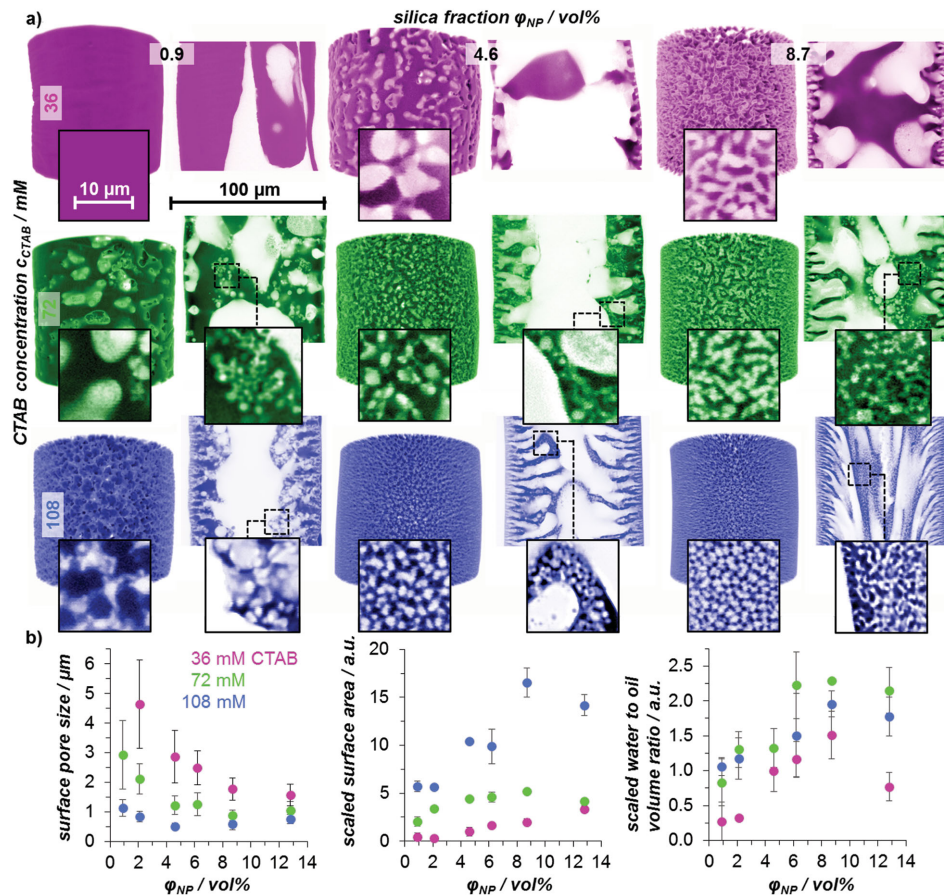


Figure 3. Tunability of fiber surface and internal structures. a) False colored 3D-reconstructions of fiber segments from confocal z-stacks and corresponding equatorial slices (for a more clear visualization of the internal fiber structure, see SI-video 6, Supporting Information). Insets correspond to magnified sections of the fiber surface and internal structure; pink, green, and blue regions correspond to polymerized HDA, whereas white domains are filled with water. Fiber internal structures range from separated-voids ($c_{\text{CTAB}} = 36 \times 10^{-3} \text{ M} / \phi_{\text{NP}} = 0.046$ and 0.087 , and $c_{\text{CTAB}} = 72 \times 10^{-3} \text{ M} / \phi_{\text{NP}} = 0.009$), to interconnected-voids with finger-like shapes ($c_{\text{CTAB}} = 72 \times 10^{-3} \text{ M} / \phi_{\text{NP}} = 0.087$, $c_{\text{CTAB}} = 108 \times 10^{-3} \text{ M} / \phi_{\text{NP}} = 0.046$ and 0.087), to a continuous channel extending throughout the fiber ($c_{\text{CTAB}} = 72 \times 10^{-3} \text{ M} / \phi_{\text{NP}} = 0.046$, $c_{\text{CTAB}} = 108 \times 10^{-3} \text{ M} / \phi_{\text{NP}} = 0.009$). b) Surface pore size, surface area of the fibers, and water-to-oil domain volume ratio as a function of ϕ_{NP} and c_{CTAB} . Here, the color code of the data points corresponds to the color of the fiber segments in (a). The water-to-oil ratio and volume specific surface area in the fibers are estimated from 2D image analysis of the equatorial slices (see the Supporting Information) and normalized by the value obtained from the accurate 3D analysis of a bijel fiber with $\phi_{\text{NP}} = 0.046$ and $c_{\text{CTAB}} = 36 \times 10^{-3} \text{ M}$. Error bars correspond to standard deviations of five measurements. Figure S18, Supporting Information, shows the structure dependence on c_{CTAB} and ϕ_{NP} for fibers prepared with DEP as the oil phase.

microparticles, fibers, and membranes via STRIPS using ternary liquid mixtures. We verify that the resulting fibers are indeed bicontinuous by demonstrating transport of molecules of differing polarity within the structure. STRIPS provides several advantages that make it a highly translatable technique for bijel formation. Compared to the conventional method that uses binary liquid mixtures, wide varieties of immiscible liquid combinations can be used for bijel preparation. The fast quenching of the ternary mixture by STRIPS allows for the formation of hierarchical and asymmetric microstructures with submicron features, which expands the potential of bijels in various applications. Bijels formed via STRIPS can be produced continuously; STRIPS-bijel production can likely be readily scaled up because of its similarity to processes that have been used for mass production of solid membranes. Moreover, STRIPS could potentially be extended to 2D or 3D printing to obtain complex bijel superstructures for desired applications. Our demonstration of biphasic transport

within the bijel structure could be also extended to induce continuous reaction and separation through interfacial catalysis and interphase mass transfer. Our current investigation focuses on understanding and tailoring the mechanical properties of STRIPS bijels, which will be critical for their practical applications.

Experimental Section

Materials: SiO_2 nanoparticles (Ludox TMA, 22 nm), CTAB (BioUltra >99%), hexanedioldiacrylate (HDA, technical grade, 80%), diethylphthalate (DEP, 99.5%), butylacrylate (BA), Rhodamine 110, Nile Red, 2-hydroxy-2-methylpropiophenone (HMP) are purchased from Sigma-Aldrich and used as received. Pure water and pure ethanol 200 proof (>99.5%) are used for all experiments.

Ternary Liquid Mixture Preparation: The ternary liquid mixture comprises five main components: (i) pure ethanol, (ii) a solution of cetyltrimethylammonium bromide (CTAB) in ethanol ($200 \times 10^{-3} \text{ M}$), (iii) a

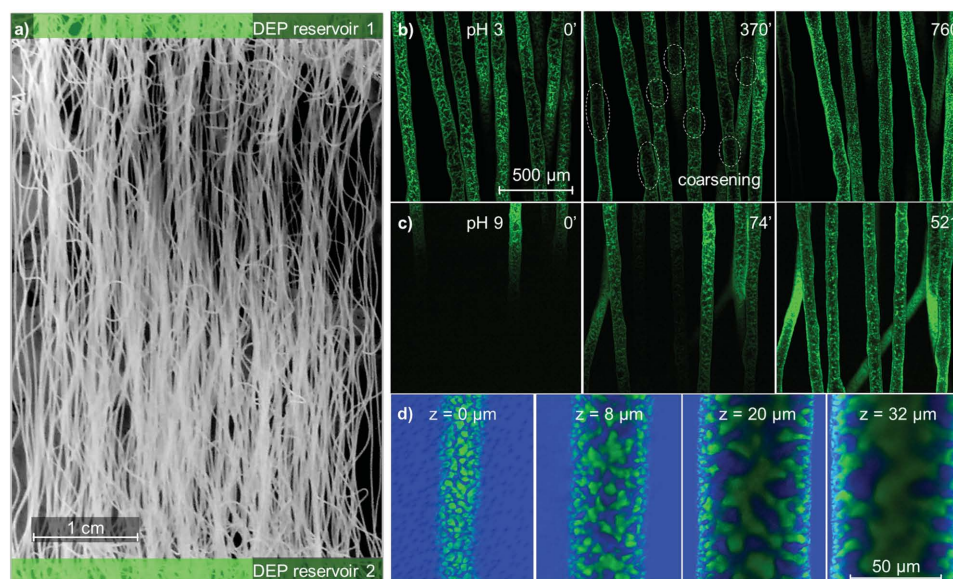


Figure 4. Biphasic mass transfer in a bundle of stable bijel fibers. a) Photograph of manually aligned fibers connected to two DEP reservoirs (represented schematically as green shaded regions at either end of the fibers). Alignment was achieved by moving outlet of the capillary device in Figure 1b side-to-side inside a water-filled petri dish. b) Confocal scanning image time series showing the coarsening of the fluorescently labeled oil domains at pH 3. c) Confocal scanning image time series showing the stability of fibers at pH 9; the diffusion of a hydrophobic fluorescent dye Nile Red throughout the fibers (green). Numbers in the upper right corner of each panel denote time in minutes (see also SI-video 7, Supporting Information). d) Confocal scanning z-stack showing the distribution of the fluorescent dye Nile red (green) in the oil phase and Rhodamine 110 (blue) in the water phase of a fiber and the continuous water phase. Numbers on top correspond to the z-position from the upper surface of the fiber.

suspension of Ludox TMA (22 nm SiO₂ nanoparticles, pH 3), (iv) pure water, and (v) oil (in our experiments HDA, BA or DEP). To prepare a solution for the generation of polymerized bijel fiber (5 mL with example composition: 70.5 × 10⁻³ M CTAB, 3 vol% silica, 0.42 wt% HMP, 41.7 vol% HDA, 41.7 vol% ethanol solution, 13.6 vol% water suspension), we add: HDA (2.06 mL), pure ethanol (0.42 mL), CTAB in ethanol (200 × 10⁻³ M, 1.67 mL), HMP (0.021 mL), Ludox TMA (18.2 vol%, 0.755 mL), and water (0.075 mL). Simple shaking of such a mixture is enough to produce a clear homogeneous solution with well dispersed silica nanoparticles. To prepare ternary mixtures with high φ_{NP} (>5 vol%), after mixing the components, we immerse the vial in an oil bath (130 °C) to evaporate water and ethanol under nitrogen flow and intense stirring. Subsequently, we add additional silica suspension (18.2 vol%), ethanol, and water to obtain mixtures of desired compositions.

STRIPS Bijel Fiber Formation: The continuous aqueous phase for bijel formation is a CTAB solution (1 × 10⁻³ M, pH 3.0). To generate bijel microparticles and fibers, we use a device made of a glass capillary (20–300 μm in diameter) aligned concentrically in a second glass capillary (300–1500 μm). To prevent undesirable adhesion of the ternary mixture to the glass capillaries, we coat all glass capillaries with polydiallyldimethylammonium chloride (PDADMAC), which is achieved by flowing a solution of polyDADMAC (1 wt%) and NaCl (0.5 M) over the capillaries. Capillaries are washed with a copious amount of water after PDADMAC modification. The ternary mixture and the continuous aqueous phase are pumped into the capillaries by means of two syringe pumps. The two phases flow in the same direction. The outer continuous phase extracts ethanol from the ternary phase, inducing phase separation. Alternatively, fiber could also be extruded into a stagnant bath of the aqueous phase. However, the outer flow helps to align the fiber and ensure uniform mass transfer. The distance between the tip of the inner capillary and the end of the outer capillary can be varied between a few millimeters up to several centimeters. Bijel microparticles and fibers can be collected by placing the end of the capillary device in a bath of water. Bijel fibers could also be aligned on a surface by moving the collection vessel (e.g., petri dish) side-to-side during collection as shown in SI-video 8, Supporting Information. To prepare photopolymerized bijel structures,

a ternary mixture with a monomer (e.g., HDA) and a photoinitiator HMP (0.1–1.0 wt% of the monomer mass) is prepared. Bijel structures, collected in a vessel, are subsequently exposed to high intensity UV light (wavelength = 340 nm, and intensity = 20 W m⁻²) for 3 min.

STRIPS Bijel Membrane Formation: A planar 0.5 mm thick polystyrene plate is immersed in a ternary liquid mixture (c_{CTAB} = 108 × 10⁻³ M, φ_{Silica} = 8.7 vol%). The plate is taken out by means of a pair of tweezers and subsequently immersed into a water bath (1 × 10⁻³ M CTAB, pH 3).

Dye Diffusion in Aligned Fibers: A microscope slide is glued with UV-glue in the center of a polystyrene petri dish. The dish is filled afterward with a polyDADMAC solution to coat the microscope slide with the cationic polymer. After excessive washing with pure water, the slide is filled with the continuous water phase (1 × 10⁻³ M CTAB). Diethylphthalate with Nile Red is then spread underwater at the edge of the microscope slide onto the polystyrene surface. We then move the outlet of the glass capillary device above the microscope slide and the spread DEP from side to side to obtain aligned fibers connected to liquid DEP. With the confocal microscope we follow the diffusion of Nile red through the continuous oil phase of the fibers (laser excitation 480 nm, Nile Red emission 600–700 nm). For observing the diffusion in the water phase, we prepare fibers with HDA in the continuous phase (20 vol% glycerol to increase the refractive index). We directly add a small amount of Rhodamine 110 powder to the continuous water phase, which is then excited with a laser (480 nm) and its emission (500–550 nm) is observed.

Supporting Information

Supporting Information is available from the Wiley Online Library or from the author.

Acknowledgements

This work was supported by NSF CBET-1449337 and Penn MRSEC DMR11-20901 through the NSF. M.F.H. was supported by the

German Research foundation (DFG) under Project No.: HA 7488/1–1. The authors also like to thank Prof. Randall Kamien (University of Pennsylvania) for helpful discussion and Prof. Ivan Dmochowski (University of Pennsylvania) for access to the confocal microscope.

Received: July 20, 2015

Revised: September 1, 2015

Published online: October 5, 2015

-
- [1] R. Aveyard, B. P. Binks, J. H. Clint, *Adv. Colloid Interfaces* **2003**, 100, 503.
- [2] M. F. Haase, D. O. Grigoriev, H. Moehwald, D. G. Shchukin, *Adv. Mater.* **2012**, 24, 2429.
- [3] J. Frelichowska, M. A. Bolzinger, J. Pelletier, J. P. Valour, Y. Chevalier, *Int. J. Pharm.* **2009**, 371, 56.
- [4] C. C. Berton-Carabin, K. Schroën, *Annu. Rev. Food. Sci. Technol.* **2015**, 6, 263.
- [5] K. Stratford, R. Adhikari, I. Pagonabarraga, J.-C. Desplat, M. E. Cates, *Science* **2005**, 309, 2198.
- [6] E. M. Herzig, K. A. White, A. B. Schofield, W. C. K. Poon, P. S. Clegg, *Nat. Mater.* **2007**, 6, 966.
- [7] M. E. Cates, P. S. Clegg, *Soft Matter* **2008**, 4, 2132.
- [8] T. Ngai, S. Bon, *Particle-Stabilized Emulsions and Colloids: Formation and Applications*, Royal Society of Chemistry, Cambridge, UK **2015**, Ch. 6.
- [9] A. J. Bray, *Adv. Phys.* **1994**, 43, 357.
- [10] F. Jansen, J. Harting, *Phys. Rev. E* **2011**, 83, 046707.
- [11] S. Crossley, J. Faria, M. Shen, D. E. Resasco, *Science* **2010**, 327, 68.
- [12] J. W. Tavacoli, J. H. J. Thijssen, A. B. Schofield, P. S. Clegg, *Adv. Funct. Mater.* **2011**, 21, 2020.
- [13] L. Bai, J. W. Fruehwirth, X. Cheng, C. W. Macosko, *Soft Matter* **2015**, 11, 5282.
- [14] M. N. Lee, A. Mohraz, *Adv. Mater.* **2010**, 22, 4836.
- [15] J. A. Witt, D. R. Mumm, A. Mohraz, *Soft Matter* **2013**, 9, 6773.
- [16] M. N. Lee, A. Mohraz, *J. Am. Chem. Soc.* **2011**, 133, 6945.
- [17] a) M. Pera-Titus, L. Leclercq, J. M. Clacens, F. De Campo, V. Nardello-Rataj, *Angew. Chem.* **2015**, 127, 2028; b) M. Pera-Titus, L. Leclercq, J. M. Clacens, F. De Campo, V. Nardello-Rataj, *Angew. Chem. Int. Ed.* **2015**, 54, 2006.
- [18] K.-V. Peinemann, V. Abetz, P. F. W. Simon, *Nat. Mater.* **2007**, 6, 992.
- [19] S. A. Vitale, J. L. Katz, *Langmuir* **2003**, 19, 4105.
- [20] M. Bendová, K. Rehak, J. Matouš, J. P. J. Novák, *Chem. Eng. Data* **2001**, 46, 1605.
- [21] a) M. F. Haase, J. Brujic, *Angew. Chem.* **2014**, 126, 11987; b) M. F. Haase, J. Brujic, *Angew. Chem. Int. Ed.* **2014**, 53, 11793.
- [22] J. M. Park, R. Mauri, P. D. Anderson, *Chem. Eng. Sci.* **2012**, 80, 270.
- [23] B. P. Binks, J. A. Rodrigues, W. J. Frith, *Langmuir* **2007**, 23, 3626.
- [24] I. Akartuna, A. R. Studart, E. Tervoort, U. T. Gonzenbach, L. J. Gauckler, *Langmuir* **2008**, 24, 7161.
- [25] B. P. Binks, J. A. Rodrigues, *Langmuir* **2007**, 23, 7436.
- [26] Z. Hu, S. Ballinger, R. Pelton, E. D. Cranston, *J. Colloid Interfaces Sci.* **2015**, 439, 139.
- [27] J. Wang, F. Yang, C. Li, S. Liu, D. Sun, *Langmuir* **2008**, 24, 10054.
- [28] J. Wang, G. Liu, L. Wang, C. Li, J. Xu, D. Sun, *Colloids Surface A* **2010**, 353, 117.
- [29] M. N. Lee, J. H. J. Thijssen, J. A. Witt, P. S. Clegg, A. Mohraz, *Adv. Funct. Mater.* **2013**, 23, 417.
- [30] G. R. Guillen, Y. Pan, M. Li, E. M. V. Hoek, *Ind. Eng. Chem. Res.* **2011**, 50, 3798.
- [31] A. Skrzecz, D. G. Shaw, A. Maczynski, *J. Phys. Chem. Ref. Data* **1999**, 28, 983.
- [32] E. Sanz, K. A. White, P. S. Clegg, M. E. Cates, *Phys. Rev. Lett.* **2009**, 103, 255502.